Atomic energy loss corrections for (p,n) and (p,γ) nuclear reaction energies

P.A. Amundsen
Institute of Mathematics and Natural Sciences, Høgskolesenteret i Rogaland, Stavanger, Norway

P. H. Barker
Physics Department, Auckland University, Auckland, New Zealand
(Received 27 January 1994)

The probability of excitation of atomic electrons during various nuclear reactions has been calculated. Appropriate corrections to some experimentally determined threshold and resonance energies are given.

PACS number(s): 61.80.Ed, 61.80.Mk, 21.10.Dr, 23.20.Lv

INTRODUCTION

In recent years, considerable effort has been put into the precise measurement of nuclear reaction energies, particularly of those nuclear Q values which allow the extraction of parameters relevant to Fermi superallowed beta decay. The quoted accuracy of both (p,γ) resonance energies [1–3] and (p,n) threshold energies [4,5] has approached or even surpassed 100 eV, but so far, except in one case [12], no attempt has been made to take into account the effects of energy loss to atomic electrons, even though it is not obvious that such effects would be negligible.

The present work reports calculations of energy loss probabilities to individual atomic subshells for the particular (p,n) and (p,γ) reactions which either have been investigated or are likely to be, in the course of the superallowed Fermi decay program. In addition, the size of the apparent energy shift in the various extracted resonance and threshold energies is calculated, and the sensitivity to the actual method of analysis of the experimental data is explored. Finally, the effects on some $^{27}\mathrm{Al}(p,\gamma)$ resonances and on the $^{27}\mathrm{Al}(p,n)$ threshold are quoted. Although these last will probably never be needed for any absolute mass difference or Q-value determination, they are commonly used for precise accelerator energy calibrations, and have recently been remeasured [6].

ELECTRON EXCITATION PROBABILITIES

The theoretical description of atomic processes during nuclear scattering is greatly facilitated by the fact that the atomic and nuclear reactions are well separated in space. This means that the atomic processes can be accurately described using only asymptotic nuclear wave functions. This leads to a well-defined first-order atomic perturbative approach, the "Blair theory," for describing atomic excitation/ionization during elastic (resonant) nuclear reactions (Refs. [7–10]). The formalism applies equally well to discrete excitation and ionization, but the latter process is the dominant cause of energy loss for the reactions we are interested in (see below). The generalization of this theory to charge-changing reactions like the (p,n) and (p,γ) is straightforward [11]. This generalized theory extends the sudden approximation, approximately corrected for K-shell Coulomb ionization, in the form introduced by Feagin, Merzbacher, and Thompson [12–14].

For conceptual clarity we shall initially consider the general case of a projectile of charge Z_P causing a nuclear reaction with the emission of an ejectile of charge Z_E. It is convenient to define the atomic energy loss distribution dP_{fi}/dE_f such that the total *atomic* energy loss during a collision can be written

$$\Delta E_A = \Delta E_i + \Delta E^* + E_R$$
$$= \Delta E_i + \int_0^\infty (E_f - E_i)\frac{dP_{fi}}{dE_f}dE_f + \tfrac{1}{2}Nm_e v_R^2 , \quad (1)$$

supplemented with the corresponding sum over final states in the bound spectrum. Here $\Delta E_i = E(Z',N) - E(Z,N)$ is the atomic ground-state energy shift, $E(Z,N)$ being the energy of an N-electron atom/ion, and $Z' = Z + \Delta Z = Z + Z_P - Z_E$. Furthermore, $E_f - E_i$ is the excitation energy of the *daughter* atom/ion relative to its ground state, while v_R is the recoil velocity of the atom after the collision and m_e the electron mass. The explicit inclusion of the electronic recoil energy E_R in Eq. (1) means that the kinetic energy of the ejected electron, included in the final state energy E_f, should be taken with respect to the *recoiling* nucleus. This term is conveniently taken care of by using *atomic* masses instead of the nuclear masses in *all* kinematical relations, and will thus not be considered explicitly in the following. This splitting of the atomic energy loss corresponds to describing the process in a coordinate system anchored to the recoiling nucleus, which is convenient since it allows for the simplest description of the atomic states [15,16,13]. This description is of course unitarily equivalent to the space-fixed description, as used by Feagin, Merzbacher, and Thompson [12].

Within first-order perturbation theory where the perturbations are caused by one-electron operators, the ini-

tial and final electronic (many-electron) states, $|\Psi_i\rangle_Z$ and $|\Psi_f\rangle_{Z'}$, can differ at most by a single orbital. For a charge-changing nuclear reaction one must in addition include the contribution caused by these states being eigenstates of different Hamiltonians. Assuming the atomic wave function to be a single Slater determinant of mutually orthogonal one-electron orbitals, the atomic energy loss distribution (which conventionally—but inaccurately—is called the differential ionization probability in the atomic physics literature) summed over all initial states in a full atomic shell and all final magnetic substrates can be written (our notation generalizes that of Ref. [10] corrected for some unfortunate typographical errors)

$$\frac{dP_{fi}}{dE_f} = \frac{1}{|T(K_P,K_E,\theta)|^2}\sum_{l,m}\left|\sqrt{\frac{4\pi}{2l+1}}Y_l^m(\theta,0)\right.$$
$$\times\mathcal{R}_{E,l}^{fi}T(K_P,K_E,\theta)$$
$$\left.+(-1)^l\delta_{m,0}\mathcal{R}_{P,l}^{fi*}\sqrt{\frac{K_PK_E}{K'_PK'_E}}T^*(K'_P,K'_E,\theta)\right|^2. \quad (2)$$

Here the subscripts $I = P, E$ refer to the projectile and the ejectile, respectively, v_I is the corresponding velocity, $K_I = \tilde{M}_I v_I$ the momentum ($\tilde{M}_I$ being the reduced *atomic* mass), and E_I the energy. Also

$$K'_I = \sqrt{\frac{E_I - (E_f - E_i)}{2\tilde{M}_I}} \quad (3)$$

is the momentum of the projectile/ejectile after having ejected an electron, so that

$$q_I = K_I - K'_I \approx \frac{E_f - E_i}{v_I} \quad (4)$$

is the minimum momentum transfer compatible with an energy transfer of $E_f - E_i$ in a purely *two-body* collision. Furthermore, θ is the emission angle of the ejectile with respect to the projectile and $T(K,\theta)$ the T-matrix element for the *nuclear* process of interest. If several nuclear final states are involved, one has to sum (2) incoherently over these. Furthermore, the following notation has been introduced:

$$\begin{aligned}
\mathcal{R}_{I,l}^{fi} &= i^l(P_{I,l}^{fi} + iQ_{I,l}^{fi}),\\
P_{I,l}^{fi} &= C_{I,l}^{fi}\int_{q_I}^{\infty}\frac{ds}{s}F_l^{fi}P_l\left(\frac{q_I}{s}\right),\\
Q_{I,l}^{fi} &= \frac{2}{\pi}C_{I,l}^{fi}\left[\mathcal{P}\int_0^{\infty}\frac{ds}{s}F_l^{fi}Q_l\left(\frac{q_I}{s}\right) - \hat{Q}_{I,l}^{fi}\right],\\
C_{I,l}^{fi} &= \frac{Z_Ie^2}{v_I}\sqrt{(2J_f+1)(2l+1)(2J_i+1)}\\
&\quad\times\begin{pmatrix} J_f & l & J_i\\ \frac{1}{2} & 0 & -\frac{1}{2}\end{pmatrix}\tfrac{1}{2}[1+(-1)^l\Pi_i\Pi_f],\\
F_l^{fi} &= \langle j_l(sr)\rangle_{fi}.
\end{aligned} \quad (5)$$

Here $\mathcal{P}$ denotes the principal value integral, P_l and Q_l are Legendre functions of the first and second kinds, respectively, j_l is a spherical Bessel function, and $\langle X\rangle_{fi}$ denotes a *radial* matrix element of an operator X between initial and final atomic orbitals of total angular momentum J_i (parity Π_i) and J_f (parity Π_f), while $(:::)$ denotes Wigner's 3-j symbol.

With the exception of $\hat{Q}_{I,l}^{fi}$, the contributions to (5) arise from the Coulomb potential of the projectile/ejectile only. The additional terms are given by

$$\hat{Q}_{I,l}^{fi} = \begin{cases} \frac{1}{q_I}\left\langle\frac{1}{r}\right\rangle_{fi}, & l=0,\\ \frac{m_e\tilde{M}_Iv_I^2}{3M_IZ_Ie^2}\langle r\rangle_{fi}, & l=1,\\ 0, & l\geq 2.\end{cases} \quad (6)$$

The two nonvanishing terms are the dominating ones in the asymptotic high energy limit, and are the only terms surviving in the (perturbative) sudden approximation [12,14] (in addition to E_R). Each of them has a simple physical interpretation. The $l = 0$ term ("the sticking amplitude") simply arises from the nonorthogonality of $|\Psi_f\rangle_{Z'}$ and $|\Psi_i\rangle_Z$ for a charge-changing collision. To see this, notice that the difference between the initial and final state atomic Hamiltonians is simply

$$\Delta H = -\Delta Ze^2\sum_{j=1}^{N}\frac{1}{r_j}, \quad (7)$$

the sum running over all the atomic electrons. Thus we have an overlap contribution to the transition amplitude given by $(i \neq f)$

$$\begin{aligned}
{}_{Z'}\langle\Psi_f|\Psi_i\rangle_Z &= \frac{1}{E_f - E_i}{}_{Z'}\langle\Psi_f|\Delta H|\Psi_i\rangle_Z\\
&= -\frac{\Delta Ze^2}{E_f - E_i}\sum_{i=1}^{N}{}_Z\left\langle\Psi_f\left|\frac{1}{r_i}\right|\Psi_i\right\rangle_Z\\
&\quad+\mathcal{O}((\Delta Z)^2)\\
&= -\frac{\Delta Ze^2}{E_f - E_i}\left\langle f\left|\frac{1}{r}\right|i\right\rangle + \mathcal{O}((\Delta Z)^2),
\end{aligned} \quad (8)$$

where $|i\rangle$ and $|f\rangle$ are the single pair of one-particle orbitals by which $|\Psi_i\rangle_Z$ and $|\Psi_f\rangle_Z$ differ. This amplitude yields precisely $\hat{Q}_{I,l}^{fi}$.

On the other hand, one has that this term alone gives rise to an energy loss ΔE_Z^* [since ΔE_i is included explicitly in Eq. (1), it is not included in ΔE_Z^*]:

$$\begin{aligned}
\Delta E_Z^* &= \sum_f(E'_f - E_i)|{}_{Z'}\langle\Psi_f|\Psi_i\rangle_Z|^2 - \Delta E_i\\
&= \sum_f{}_Z\langle\Psi_i|\Delta H|\Psi_f\rangle_{Z'}\,{}_{Z'}\langle\Psi_f|\Psi_i\rangle_Z - \Delta E_i\\
&= -\Delta Ze^2\sum_{j=1}^{N}{}_Z\left\langle\Psi_i\left|\frac{1}{r_j}\right|\Psi_i\right\rangle_Z - \Delta E_i\\
&= \Delta Z\left(\frac{\partial E(Z,N)}{\partial Z}\right)_N - E(Z+\Delta Z,N) + E(Z,N)\\
&= -(\Delta Z)^2\left(\frac{\partial^2E(Z,N)}{\partial Z^2}\right)_N + \mathcal{O}((\Delta Z)^3).
\end{aligned} \quad (9)$$

Here the Hellmann-Feynman theorem is used in the next to the last step. This elegant result is due to Wilkinson [14], who also pointed out that it can be used to extract good approximations to ΔE_Z^* from tabulated values of atomic ground-state energies. However, since the sticking amplitude adds coherently to the Coulomb excitation amplitude in Eq. (4), we shall use the latter expression as a starting point for our numerical work.

The $l = 1$ term in Eq. (5) also has a simple physical interpretation: It is the amplitude for ionization due to the recoil of the nucleus. This term is actually present in the leading order sudden approximation [12], but has been mostly neglected since it causes dipole transitions only. However, this term is always at least comparable to the Coulomb dipole contribution for zero impact parameter [15], and so must be included together with the Coulomb amplitudes.

The structure of our basic formula, Eq. (2), is readily interpreted: The energy loss probability is a coherent superposition of two amplitudes. One contains $\mathcal{R}_{P,l}^{fi}$, and describes ionization caused by the incoming projectile, so that the nuclear reaction takes place at a reduced incident momentum K_P', as described by $T^*(K_P', K_E', \theta)$ (amplitude for "ionization before the nuclear reaction"). The second amplitude describes ionization by the ejectile ($\mathcal{R}_{E,l}^{fi}$), and hence the nuclear reaction takes place at the full incident momentum K_P (amplitude for "ionization after the nuclear reaction").

For the purpose of the present investigation, we are only interested in neutral ejectiles (n, γ), so $Z_E = 0$, and hence there is no ionization by the ejectile, except that which is caused by the recoil. Moreover, as long as we are only interested in (p, γ) and (p, n) reactions close to the neutron threshold, the recoil of the ejectile is far too feeble to cause any significant ionization. We can thus safely neglect the first amplitude in Eq. (2), which simplifies both the computational work and the analysis of the experiments.

We have evaluated formulas (2)–(6) using a rewritten version of the code previously described in Ref. [10]. The atomic orbitals are relativistic one-electron eigenfunctions derived from optimized effective atomic (OPM) potentials [17]. The use of relativistic electron wave functions gives only a minor improvement for systems as light as those of present interest, but neither does it increase the calculational complexity. The use of wave functions derived from a realistic atomic potential is, on the other hand, crucial for an accurate description of the outer atomic shells.

The purely numerical accuracy of our calculations is estimated to be better than 5%. It is essentially limited by the stability of the integration of the various oscillating integrands in Eq. (5), in particular for outer shell wave functions with many radial nodes. However, the actual accuracy of the calculations is set by the limitations of the theory employed. One obvious deficiency is our neglect of discrete excitations. As a matter of fact, it has long been known that (discrete) Coulomb excitations give only a very minor contribution to ion-induced inner shell vacancy production cross sections [18]. It is also easily seen to be true in the sudden approximation: The overlap amplitude (8) ${}_{Z'}\langle\Psi_f|\Psi_i\rangle_Z$ tends to have its maximum when the momentum distributions in the two wave functions peak in the same range, i.e., at comparable *kinetic* energies. Thus the electrons tend to be ejected well into the continuum. This can alternatively be seen from Wilkinson's formula (9), applied to a single-electron ion, so that $E(Z,1) = -Z^2e^2m_e/2$ and $E_Z^* = (\Delta Z)^2 m_e e^2$. For hydrogenic ground-state wave functions the total excitation probability (including ionization) in the sudden approximation becomes

$$P_Z^* = 1 - |{}_{Z'}\langle i|i\rangle_Z|^2 = 1 - \frac{(1-\Delta Z/Z)^{3/2}}{(1-\Delta Z/Z)^3} \xrightarrow[\Delta Z/Z\to 0]{} \frac{3}{8}\left(\frac{\Delta Z}{Z}\right)^2 . \quad (10)$$

Thus the average energy transferred to an excited electron becomes

$$\langle E_f - E_i\rangle = E_Z^*/P_Z^* \xrightarrow[\Delta Z/Z\to 0]{} \tfrac{8}{3}Z^2 m_e e^2 = \tfrac{16}{3}|E(Z,1)| .$$

Thus the typical electron contributing to the atomic energy loss is ejected well into the continuum. The result remains qualitatively correct for more realistic wave functions.

As for other restrictions on the accuracy, it should be noted that the valence electrons are not well described by uncorrelated wave functions. Also, these electrons are easily polarized by the incoming projectile, and have large ionization probabilities, so first-order perturbation theory does not work too well. On the other hand, the contribution from the outermost electrons to the total energy loss is small (< 10%), so that inaccuracies in these numbers are not likely to dramatically influence the total estimated energy loss. Only the lightest atoms ($Z \leq 10$) are exceptions to this. Thus for ^{14}N at 6.3 MeV the three valence electrons contribute some 40% of the energy loss, and all results based upon perturbative approaches should be regarded with suspicion.

In Table I we compare the results of our full calculations of E^* and Wilkinson's simple energy-independent estimates, with the second derivative in (9) approximated by second differences of tabulated neutral atom ground-

TABLE I. Comparison of ΔE^* from the present work with the estimates from Ref. [14].

Reaction	Energy (keV)	ΔE^* (present) (eV)	ΔE_Z^* (Ref. [14]) (eV)
^{14}N(p,n)	6300	164	105
^{26}Mg(p,n)	5210	88	123
^{27}Al(p,n)	5800	141	129
^{34}S(p,n)	6460	141	142
^{42}Ca(p,n)	7400	139	149
^{25}Mg(p,γ)	1380	57	123
^{25}Mg(p,γ)	1590	60	123
^{27}Al(p,γ)	990	91	129
^{27}Al(p,γ)	1320	95	129
^{33}S(p,γ)	970	93	142
^{33}S(p,γ)	1540	101	142
^{33}S(p,γ)	1990	105	142

state energies [19]. The systematics of the differences between the results of Wilkinson's simplified method [Eq. (9)] and the full calculations are easily explained, as the addition of Coulomb and recoil amplitudes have two opposite effects. The monopole excitation amplitude adds coherently to the sticking amplitude [Eq. (5)], but has the opposite sign and so reduces Wilkinson's estimate. The dipole amplitude (including recoil), on the other hand, adds coherently to these results, and thus always increases them. For slow collisions [the (p,γ) reactions] the dipole contributions are small, and the main effect is a significant reduction of the energy loss of the monopole contribution. For the faster (p,n) reactions, the dipole amplitude is large for the light target elements, but decreases rapidly in importance with increasing target Z (for fixed projectile speed).

It is seen that the simple energy-independent Wilkinson formula (9) works quite well for the higher energy (p,n) reactions (except for Al, where the contributions from the valence electrons are large, and the results sensitive to the details of the matrix elements), but not for the lower energy (p,γ) collisions.

Figure 1 shows the differential energy loss probability, dP/dE, as a function of energy loss E of a proton of energy 1.38 MeV, involved in the corresponding resonance in the ^{25}Mg(p,γ) reaction. Although P is spoken of as a probability, a better interpretation is as the expected number of ejected electrons. The obvious steps in the curve correspond to the ionization energies of the different subshells, and both the dP/dE and E axes are represented logarithmically for clarity. The integral of dP/dE over E, i.e., the number of electrons ejected per proton, is 0.773. Also shown is a similar curve for the case of protons of energy 5.20 MeV, appropriate to the ^{26}Mg(p,n) threshold measurement at that energy. The total number of electrons ejected per proton in this case is 1.048. Not shown in Fig. 1, but quoted below in Table II, is the evaluation for 1.59 MeV protons on magnesium. The curve is virtually identical to that for 1.38 MeV.

RESONANCE AND THRESHOLD YIELD CURVES

Normally, when a precise energy determination is made of a (p,γ) resonance, a narrow prominent resonance is chosen, and the yield of the resonance, often manifested as emitted gamma rays, is measured as a function of the incident proton energy, using a target which is several keV thick to the incoming beam. In the approximation that the resonance is infinitely narrow and the beam monoenergetic, this leads to a yield curve whose form resembles a step function, and the position of the resonance may be unambiguously determined.

In practice, several factors complicate this simple picture. A suitable resonance will be perhaps 100 eV wide and Lorentzian in shape. The proton beam from the accelerator will have an energy distribution which, hopefully, can be determined. In the measurements reported in Refs. [3–6], this was so, and it proved to be quite closely symmetrically Gaussian, with a width of several hundred eV. The inclusion of both of the above factors rounds the corners of the step function, but the position of the resonance may be reliably extracted by interpolating in the yield curve to find the energy at which the resonance yield is half that on the flat top.

A third effect is that due to the nonuniform energy loss of the protons as they traverse the target. That is, because the energy dependence of the cross section for the collisions of the incoming protons with the electrons of the target favors small energy losses, a "snapshot" of the proton energy distribution at any moment would show, not a uniform distribution from the incoming to the out-

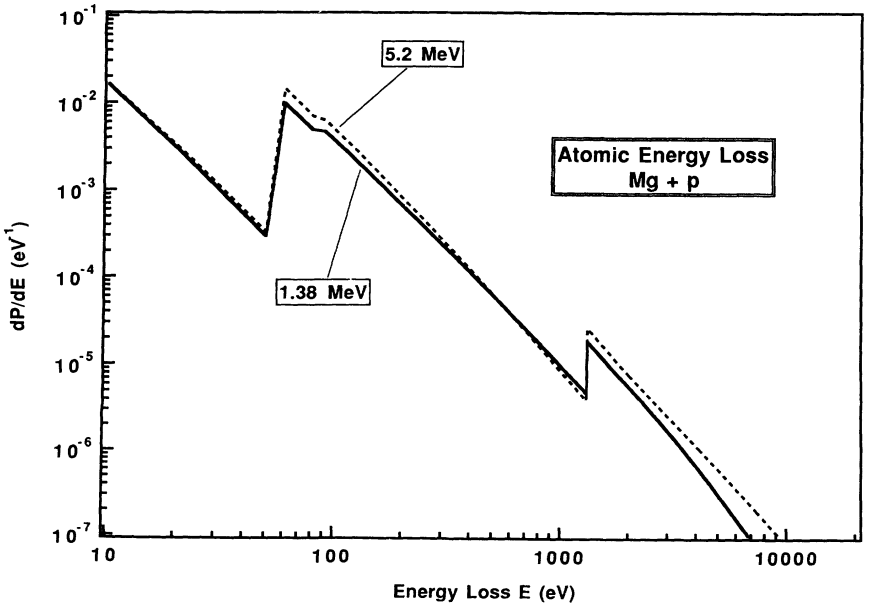

FIG. 1. Differential energy loss curves for protons incident on magnesium. The dashed curve is for the case of ^{26}Mg(p,n) with $E_p = 5.2$ MeV, and the continuous curve is for ^{25}Mg(p,γ) with $E_p = 1.38$ MeV.

going energy, but rather an excess of particles near the higher energy. This has an asymmetric effect on the yield curve, producing the traditional "Lewis peak" [20], and a procedure for extraction of the resonance energy must be determined.

A fourth process which should not be neglected, and which is the subject of the present report, is the ejection of a bound electron from the atom in which the nuclear reaction is taking place, which makes it seem as though more energy is needed for the nuclear process than is actually the case. Since the correction for this, as for the three previously mentioned processes, is always of the order of 100 eV or less, the evaluation of it will be considered independently of the others. As examples of the two different kinds of reaction, the analysis of the yield curves for one (p,γ) resonance and one (p,n) threshold will be considered in the next section.

^{25}Mg(p,γ) AT $E_p = 1.38$ MeV

In practice, a simple and reliable procedure for extracting a resonance position from a thick target yield curve is to establish the levels of the (assumed) flat top of the curve, Y_T, and of the background below the resonance, Y_B. Then the position of the resonance itself is the energy at which the yield is $(Y_B + Y_T)/2$. If the resonance has a Breit-Wigner shape and the beam energy distribution is symmetrically Gaussian, this procedure is unaffected. Some account must then be taken of the Lewis peak, but that will not be dealt with here.

In Fig. 2, the dashed curve shows artificial data, generated at 10 eV intervals by convolving a step function with a Lorentzian of full width at half maximum (FWHM) 100 eV. The ratio of the resonance height to flat background is 5:1, which is typical for the cases to be quoted, and the position of the resonance has been set at a relative proton energy of 0 eV. The continuous curve shows the effect of the further folding in of the appropriate atomic energy loss curve of Fig. 1. If the half-height is now established, it is found that there has been a shift to a slightly higher energy, as expected, in this case by 95 eV.

The shift quoted above was calculated as if each interacting proton ejected one electron, for which the energy loss probability distribution was given by Fig. 1. However, the total probability (the area under the continuous curve of Fig. 1) is not unity, but rather 0.77. So the correction to be applied to the resonance energy extracted from the yield curve is to subtract (0.77×95), i.e., 73 eV.

The procedure was repeated for several analysis widths ranging from ± 2 to ± 5 keV, but the shift was insensitive to this range. However, there is a slight dependence on the FWHM of the Lorentzian. For FWHM's of 14, 50, 100, and 500 eV, the corrections were 62, 68, 73, and 85 eV, respectively. Because of this and since also the data are in 10 eV steps, a conservative error of ± 30 eV is uniformly assigned to the results.

^{26}Mg(p,n) AT E_p=5.21 MeV

The cross section for a (p,n) reaction close to threshold is expected to show the energy dependency of s-wave neutron emission, i.e., $\sigma \propto (E - E_0)^{0.5}$, where E_0 is the threshold energy, and so the yield curve for a thick target has a form $\propto (E - E_0)^{1.5}$ under the assumption that the proton energy loss is uniform as it traverses the target. Consequently the analysis of a yield curve to extract the threshold energy is by employing a nonlinear least squares procedure to fit the function $Y = A(E - E_0)^{1.5} + B$ to the data, where B is a background which is assumed constant over the range of interest. For recent work [4,6], data have been analyzed over a range of from ± 2 to ± 5 keV relative to the threshold.

Unlike the case for a resonance, the three ancillary ef-

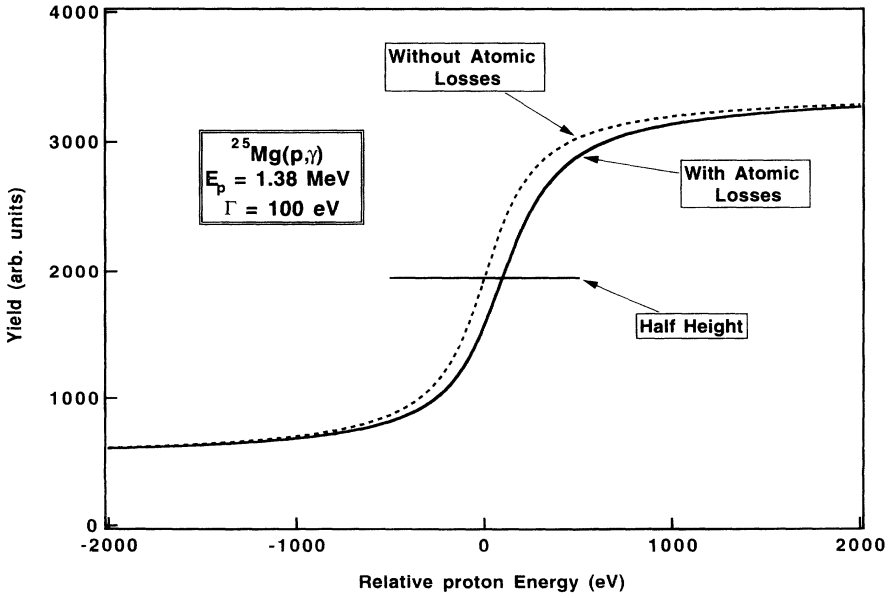

FIG. 2. Illustrating the effect of incorporation of atomic energy losses into the shape of a thick target yield curve for ^{25}Mg(p,γ) with $E_p = 1.38$ MeV and a resonance width of 100 eV.

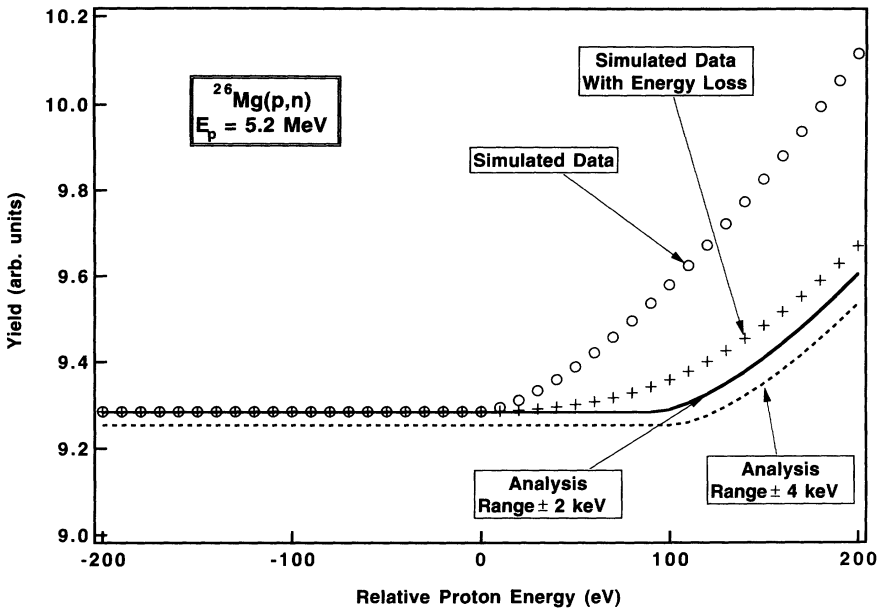

FIG. 3. Incorporation of atomic energy losses into the thick target yield curve for the ^{26}Mg(p,n) reaction near the threshold at 5.2 MeV. The dashed and continuous curves represent analyses made using two different assumptions (see text).

fects, beam energy spread, nonuniform proton energy loss, and atomic excitations, all produce an apparent threshold shift. Only the last will be considered here. In Fig. 3, circular dots indicate artificial data in 10 eV steps, generated with the functional form Y above. The crosses represent these data when the effects of the atomic excitation curve of Fig. 1 are taken into account. The threshold has been set at a relative proton energy of 0 eV. For clarity, although the data were produced over the range of $(0 \pm 5$ keV), only a small central portion is shown. The continuous and dotted curves show the best analyses, as outlined above, when the data are analyzed over the range $(0 \pm 2$ keV) and $(0 \pm 4$ keV), respectively. The threshold shifts are 93 and 102 eV. A further test of the sensitivity of the procedure outlined was performed by using finer step sizes of 1 eV, instead of 10 eV. The extracted threshold shifts were stable to 10 eV or better.

In this case, the number of electrons ejected per interacting proton, P, is 1.05, and since the results quoted in Table II are for an analysis range of (threshold ± 3 keV), the shift is the average of 93 and 102 eV multiplied by 1.05, i.e., a subtraction of (102 ± 30) eV.

TABLE II. Calculated corrections to extracted threshold and resonance energies for various reactions (see text).

Reaction	Energy (keV)	P	Correction ($-$eV)
^{14}Ni(p,n)	6300	2.83	133(70)
^{26}Mg(p,n)	5210	1.05	102(30)
^{27}Al(p,n)	5800	1.13	100(30)
^{34}S(p,n)	6460	1.41	47(30)
^{42}Ca(p,n)	7400	0.90	82(30)
^{25}Mg(p,γ)	1380	0.77	73(30)
^{25}Mg(p,γ)	1590	0.86	82(30)
^{27}Al(p,γ)	990	0.77	24(20)
^{27}Al(p,γ)	1320	0.86	44(20)
^{33}S(p,γ)	970	1.10	33(20)
^{33}S(p,γ)	1540	1.12	36(20)
^{33}S(p,γ)	1990	1.15	37(20)

RESULTS

In Table II are shown the evaluated corrections for the (p,γ) and (p,n) cases discussed in the introductory section. The resonance FWHM for the former has been taken to be 100 eV, while the range of analysis for the latter is within ± 3 keV of the threshold, although the sensitivity to both these parameters is small. As anticipated, the magnitude of the effects is small but not negligible, with the largest shifts being of order 100 eV for the (p,n) thresholds.

As particular examples of (p,γ) and (p,n) cases which are of interest in the superallowed beta decay program, some results from Refs. [3,4] may be quoted. The Q value for the beta decay of the 0^+, $T = 1$ ground state of ^{34}Cl to its analogue partner in ^{34}S may be given in terms of the difference of the neutron separation and proton separation energies, S_n and S_p, for ^{34}Cl. The latter may be measured by choosing one or more sharp, prominent resonances in the ^{33}S(p,γ) reaction and determining the resonance energies and the corresponding excitation energies. This was done several times for each of three proton energies at roughly 975, 1544, and 1995 keV, with beam energy widths of 200 ppm. The respective corrections applied for atomic excitations, as discussed in the present work, were -30, -40, and -40 eV, leading to resonance energies of 974.61(4), 1543.49(5), and 1994.86(7) keV. When these were combined with the excitation energies, final values for S_p of 5143.27(9), 5143.27(6), and 5143.34(8) keV were obtained, giving excellent agreement of 5143.29(7) keV.

The Q value for the superallowed decay of $^{26}Al^m$ to ^{26}Mg is directly given in terms of the threshold energy of the $^{26}Mg(p,n)^{26}Al^m$ reaction at around 5.21 MeV. As described in Ref. [4], this yield curve near threshold was studied six times. A typical case was from -4 to $+0.5$ keV with respect to threshold, using a beam of energy width 75 ppm, and the corrections applied for finite beam energy width, nonuniform proton energy loss, and atomic excitations were $+0.04$, $+0.06$, and -0.10 keV, respectively. The final threshold energy was determined to be 5209.46(12) keV.

CONCLUSIONS

Corrections to various extracted threshold and resonance energies of interest in studies of superallowed beta decay and for calibration purposes have been calculated and have been shown to be small, but not negligible.

ACKNOWLEDGMENTS

One of us (P.H.B.) would like to thank the Istituto Nazionale di Fisica Nucleare, Università di Firenze, Sezione di Firenze, for warm support and hospitality during the completion of this work.

[1] S. Raman, E. T. Jurney, D. A. Outlaw, and I. S. Towner, Phys. Rev. C **27**, 1188 (1983).
[2] S. W. Kikstra, Z. Guo, C. Van der Leun, P. M. Endt, S. Raman, T. A. Walkiewich, and I. S. Towner, Nucl. Phys. **A529**, 39 (1991).
[3] S. Lin, S. A. Brindhaban, and P. H. Barker, Phys. Rev. C **49**, 3098 (1994).
[4] S. A. Brindhaban and P. H. Barker, Phys. Rev. C **49**, 2401 (1994).
[5] R. E. White, H. Naylor, P. H. Barker, D. M. J. Lovelock, and R. M. Smythe, Phys. Lett. **105B**, 116 (1981).
[6] S. A. Brindhaban and P. H. Barker, Nucl. Instrum. Methods Phys. Res. Sect. A **340**, 436 (1994).
[7] J. S. Blair, P. Dyer, K. Snover, and T. A. Trainor, Phys. Rev. Lett. **41**, 1712 (1978).
[8] J. S. Blair and R. Anholt, Phys. Rev. A **25**, 907 (1982).
[9] J. M. Feagin and L. Kocbach, J. Phys. B **14**, 4349 (1981).
[10] P. A. Amundsen and K. Aashamar, Phys. Rev. B **19**, 1657 (1986).
[11] P. A. Amundsen and D. H. Jakubaßa-Amundsen, presented at the 17th International Conference on the Physics of Electronic and Atomic Collisions, Brisbane, 1991.
[12] J. M. Feagin, E. Merzbacher, and W. J. Thompson, Phys. Lett. **81B**, 107 (1979).
[13] J. M. Feagin, Phys. Lett. **107B**, 399 (1981).
[14] D. H. Wilkinson, Nucl. Instrum. Methods Phys. Res. Sect. A **335**, 172 (1993).
[15] P. A. Amundsen, J. Phys. B **11**, 3197 (1978).
[16] D. H. Jakubaßa and P. A. Amundsen, J. Phys. B **12L**, 725 (1979).
[17] K. Aashamar, T. M. Luke, and J. D. Talman, At. Data Nucl. Data Tables **22**, 443 (1978).
[18] M. C. Walske, Ph.D. thesis, Cornell University, 1951, as cited in E. Merzbacher and H. W. Lewis, in *Corpuscles and Radiation in Matter II*, edited by S. Flügge, Handbuch der Physik Vol. 34 (Springer-Verlag, Berlin, 1958), p. 166.
[19] J. P. Desclaux, At. Data Nucl. Data Tables **12**, 311 (1973).
[20] H. W. Lewis, Phys. Rev. **125**, 937 (1962).